Synthetic methodology towards ADP-ribosylation related molecular tools

Engelsma, S.B.

1 General Introduction

Introduction

During the first half of the twentieth century the significance of the phosphate esters in biochemistry was established. In 1910, Levene made the major discovery that deoxyribonucleic acids (DNA) consist of nucleosides linked together by phosphodiesters.[1] His research set a scientific foundation, that proved crucial in the elucidation of the three-dimensional structure and function of DNA in the 1950s. In the same era it was also discovered that the conversion of adenosine diphosphate to adenosine triphosphate, facilitated by pyrophosphate co-enzyme A, forms the cornerstone of cellular respiration, thereby further signifying the importance of phosphorylation in biological processes.[2] In the following decades, the number of known biochemical processes involving phosphorylation reactions rapidly expanded. For example: protein phosphorylation, a regulatory mechanism that activates or deactivates proteins, became known as the most widespread type of post-translational modification (PTM) and recognized as a key reaction in cellular signal transduction. It is now clear that phosphorylation affects all four major biomolecules – proteins, lipids, carbohydrates and nucleic acids – and plays a pivotal role in the most basic cellular functions, such as cellular energy transfer, signal transduction, protein regulation and the biosynthesis and maintenance of the genome. Considering both the relevance and vastness of these biological processes, it is not surprising that there is a growing demand for well-defined phosphorylated molecular tools that facilitate the studying of the corresponding molecular mechanisms. In addition to a fundamental understanding of normal cell function, such tools can also be effective at elucidating the molecular mechanisms behind various pathologies and help to define potential therapeutics. Synthetic organic chemistry has already proven to be invaluable for the preparation of phosphorylated molecular tools that were designed to this end. However, most natural phosphates are inherently susceptibility to hydrolysis, trans-esterification and enzymatic cleavage. This property limits their use through possible premature degradation or restricted synthetic accessibility; the latter especially when considering the chemical complexity which biomolecules tend to present.

The research described in this Thesis focuses on the development of new molecular tools intended to facilitate the study of the PTM, adenosine diphosphate ribosylation. In this context new reagents and methodologies have been developed for the synthesis of stabilized pyrophosphorylated bioisosteres.

ADP-Ribose Transferases

Adenosine diphosphate ribosylation (ADP-ribosylation) is a post-translational modification regulated by ADP-ribose transferases (ARTs), in which NAD^+ is used to transfer ADP-ribose onto a nucleophilic heteroatom of an acceptor biomolecule, with simultaneous release of nicotinamide. Mono-ADP-ribosylation (MARylation) is a highly conserved PTM that is thought to have evolved in primal prokaryotes as a cellular-defense mechanism against viruses and antimicrobial biomolecules. Most ARTs expressed by these organisms MARylate viral DNA, RNA and proteins in order to disrupt the replication cycle. Over time, however, these originally defensive ADP-ribosylating proteins mutated into bacterial toxins, giving rise to various species of pathogenic bacteria; including infamous examples such as *Bordetella pertussis* (pertussis toxin)[3], *Clostridium botulinum* (C2-toxin, C3-toxin)[4,5], *Corynebacterium diphtheria* (diphtheria toxin)[6] and *Vibrio cholera* (cholera toxin)[7]. Each ART-toxin MARylates specific key regulatory proteins of the eukaryotic host cell; a modification highly detrimental to their function. Interestingly, all ARTs expressed in eukaryotes share similar substrates, catalytic triads and a specific structural fold (known as the ART-folds) with prototypical bacterial toxins, indicating an evolutionary lineage. Based on the homology of the catalytic domain, all eukaryotic ARTs can be categorized as cholera toxin-like or diphtheria toxin-like. In humans, 21 ARTs are expressed that can be differentiated into two subfamilies: 17 poly(ADP-ribose) polymerases (PARPs) and 4 ecto-ADP-ribose transferases (ARCTs). PARPs 1 to 5 are diphtheria toxin-like, sharing the highly conserved ART-fold and the histidine-tyrosine-glutamate (HYE) motif, which facilitates the binding of NAD^+.[8] The ARCTs are cell surface enzymes that are excreted in the extracellular department.[9] They are related to cholera-toxin and make use of an alternative arginine-serine-glutamate (RSE) motif.[10] In this chapter, the discussion will be focused on the HYE-PARPs, as their role in DNA damage repair, telomere maintenance and regulation of apoptosis have highlighted these proteins of biomedical importance, most notably in relation to cancer therapy and inflammatory disorders.

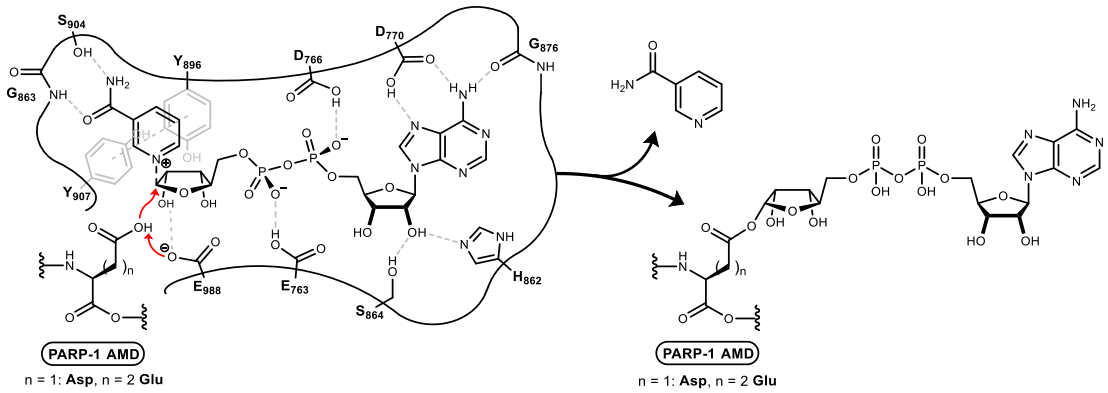

Figure 1: The catalytic mechanism of auto-ADP-ribosylation of chicken PARP-1, at the auto-modification domain (AMD). NAD^+ is shown bound in the ART-fold of PARP-1. The conserved HYE triad refers to H_{862}-Y_{896}-E_{988}. Bonding interactions are shown as grey dashed lines.[11]

PARP Mono- & Poly-ADP-Ribosylation

Both mono(ADP)ribosylation (MARylation) and the succeeding poly(ADP)ribosylation (PARylation) are modifications catalyzed by enzymes belonging to the PARP family. In contrast to their name, most PARPs are actually transferases and only capable of transferring a single mono-ADP-ribose onto a nucleophilic amino-acid at the auto-modification domain, or that of another target protein. However, at least PARP-1, PARP-2, and PARP-5a/b (tankyrases) are capable of catalyzing PARylation.[12,13] PARP-1 to 5 catalyzed ADP-ribosylation starts with the binding of NAD^+ in the ART-fold. The histidine imidazole side-chain, belonging to the conserved HYE motif (Figure 1; H_{862}-Y_{896}-E_{988}), forms a hydrogen bond with the C^2-*OH* of the NAD^+ adenosine moiety.[11] On the other end of the molecule, the electron-poor nicotinamide undergoes π-π stacking with two electron-rich tyrosine residues (Figure 1; Y_{896}-Y_{907}). These binding interactions, among various others, force a spatial orientation that instills strain on the pyridinium *N*-glycosidic bond, lowering the activation energy.[14] The exact function of HYE-glutamate during the initial ADP-ribosylation reaction is different from its role during the PARylating elongation reactions. The inherent nucleophilicity of proposed acceptor side chains, primarily those of glutamate and aspartate, is sufficient for the transfer to occur without the aid of the HYE-glutamate.[13,15,16] This theory is supported by PARP-1 mutant studies, where the absence of the Glu_{988} only gave a 3-fold decrease in auto-MARylation activity.[17] However, the HYE-glutamate is likely to facilitate the reaction through favorable hydrogen bonding and assisting in polarization of the acceptor side chain.

During PARylation, additional ADP-ribose residues are sequentially transferred onto a previously attached acceptor ADP-ribose, to form linear or branched chains of poly-ADP-ribose, consisting of up to 200 monomeric units. Most elongations proceed via α-ribosylation of NAD^+ onto the C^2-*OH* of the terminal adenosine moiety, resulting in a linear extension of the ADPR-polymer chain (Figure 2). In this instance, the HYE-glutamate residue forms a hydrogen bonding network between the acceptor C^2-*OH* of the terminal adenosine and the C^2-*OH* of the bound NAD^+ nicotinamide ribose.[18] Subsequent basic catalysis by the HYE-glutamate enables the S_N2-displacement of the nicotinamide. For PARP-1, branching of the chain irregularly occurs once every 20 to 50 ADP-ribose units, when a similar NAD^+ glycosylation reaction takes place at the C^2-*OH* of an internal ribose moiety.[19] The branching sites are ribosylated following the same linear-branching extension pattern, providing the polymer with a dendritic macrostructure.

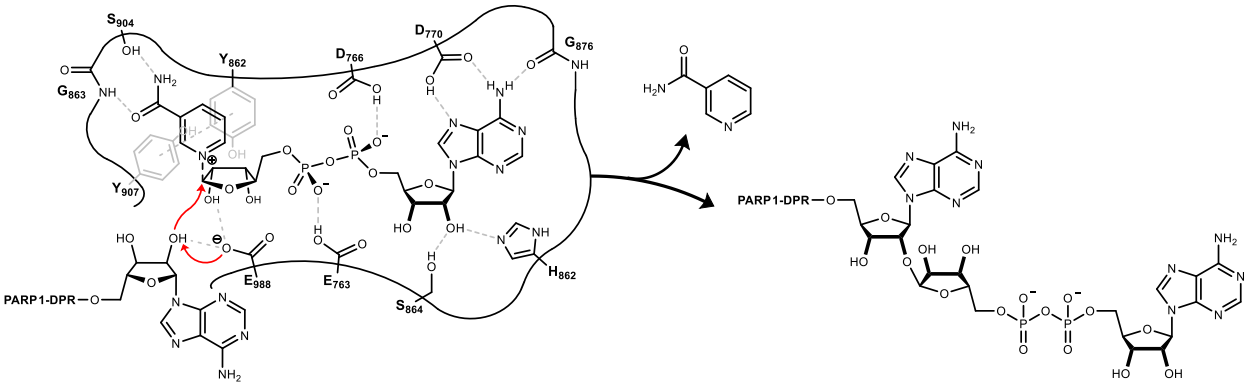

Figure 2: Catalytic mechanism of linear auto-poly-ADP-ribosylation of chicken PARP-1.

Poly-ADP-Ribosylation in DNA Repair

In eukaryotes, PARP-1, PARP-2 and PARP-3 are involved in the detection and initiation of single- and double-strand DNA break repair mechanisms, including base- and nucleotide excision repair.[20,21] Particularly PARP-1 has been subject of extensive studying, as it is the primary target for poly-ADP-ribosylation through auto-modification in response to DNA damage. The mechanism of PARP-1 activation starts by ligation of the zinc finger domains to the disconnected nucleobases at the DNA break.[22] The enforced proximity caused by this interaction allows PARP-1's Trp-Gly-Arg (WGR) domain to bind DNA, triggering a cascade of conformational changes that initiate its catalytic activity.[23] The auto-PARylation of PARP-1 promotes the recruitment of co-enzyme Histone PARylation factor 1 (HPF1), which is responsible for *trans*-ADP-ribosylation of the histones (H1, H2B and H3).[24] It is postulated that the negative charge carried by the phosphate rich poly(ADP-ribose) chains relaxes the histone and partially dissociates the DNA-bound PARP-1, creating a binding cavity for DNA repair proteins XRCC1, DNA ligase-3 and DNA polymerase-β.[25,26] After DNA repair, the PARylated proteins are regenerated through hydrolysis of the PAR-polymers by hydrolases PAR, MacroD1, MacroD2 and TARG1, completing the ADP-ribosylation cycle.

The glutamic acid and aspartate have shown to be primarily acceptor amino acids for ADP-ribosylation at the histone, and more recently lysine, arginine, cysteine and serine have also been reported.[27–30] However, data regarding the covalent poly-ADP-ribosylation of histone proteins at glutamate or aspartate residues is conflicting, and can be viewed as controversial when considering the chemical sensitivity of anomeric esters. Furthermore, non-covalent complexes between poly-ADP and the histone have also been reported.[31–33] Overall the relation between ADP-ribosylation and the target protein's acceptor amino acids and the corresponding biochemical function is poorly understood. Synthetic organic research towards well-defined mono- and poly-ADPr fragments and ADPr-functionalized oligopeptides have already proven to be incredible useful in advancing our understanding of this complex PTM.[16,34–36] The chemically diverse nature of these constructs makes them synthetically challenging. The main difficulty arises from necessity to combine several specialized subfields of organic chemistry, namely carbohydrate-, peptide- and nucleic chemistry, each associated with their own unique reactivity, tailor-made protecting groups and corresponding orthogonality. This, combined with the various labile bonds within these constructs (Figure 3), constrains the synthetic accessibility and biochemical applicability. An organic

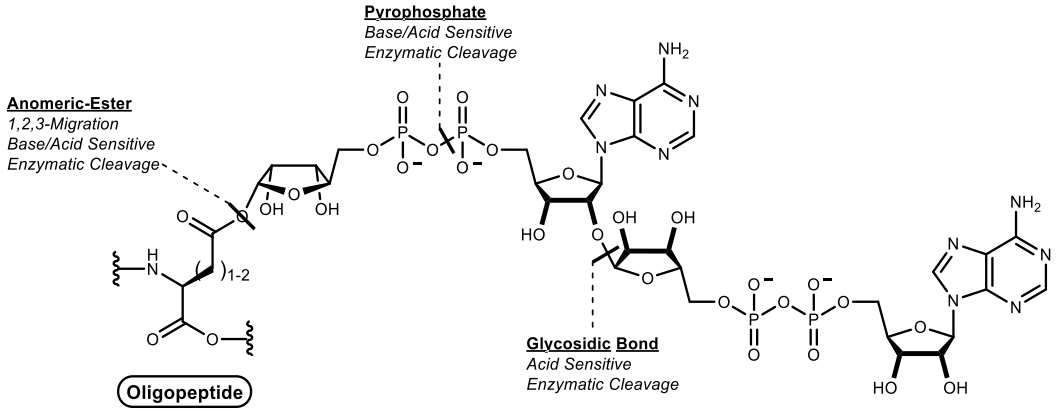

Figure 3: The general structure of an ADPr-functionalized oligopeptide, depicting the three most labile bonds; the pyrophosphate bridge, the stereospecific anomeric ester and the glycosidic bond.

chemical approach to address such limitations is to introduce chemical modifications that stabilize specific labile bonds, while, at the same time, retaining similar overall physical and chemical properties.

Stabilized NAD$^+$ Analogues

Carbanicotinamide Adenine Dinucleotide. In the 1980s scientific evidence signifying the importance of ADP-ribosylation as a regulatory PTM was rapidly being accumulated. As both the exact function and mechanism were still barely understood, there was a growing demand for molecular tools that could help to elucidate this class of PTMs.[37] In 1988, Slama and co-workers were the first to design and synthesize a stabilized analogue to this end, which came in the form of carbocyclic-nicotinamide adenine dinucleotide (*C*-NAD$^+$).[38] It was reasoned that substituting the ring oxygen of the nicotinamide riboside moiety with a methylene would stabilize the adjacent C-N bond, making it resistant to cleavage, while retaining a similar structure and polarity profile to that of natural NAD$^+$.

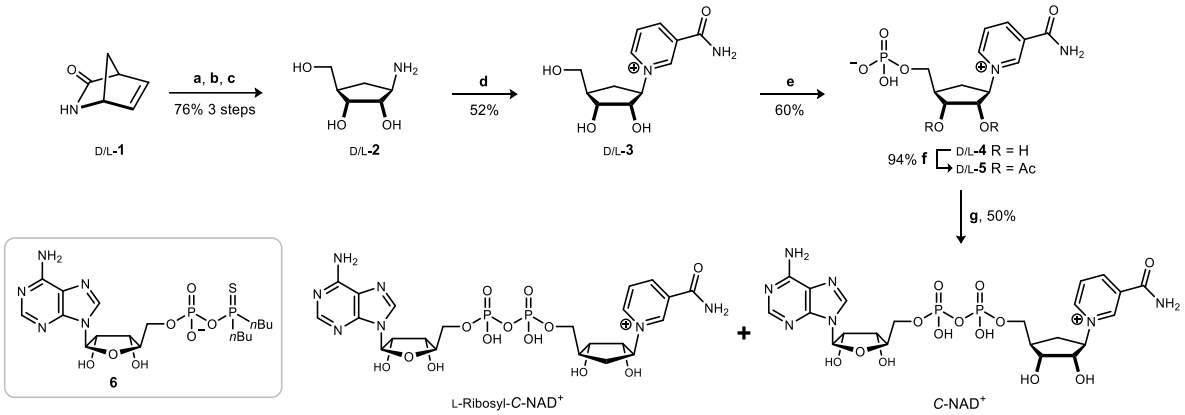

Scheme 1: Synthesis overview of *C*-NAD$^+$ as described by Slama and co-workers. Reagents and conditions: [**a**] OsO_4, MNO, *t*BuOH/H_2O, 50 °C. [**b**] HCl, MeOH. [**c**] $LiEt_3BH$, THF, 0 °C. [**d**] 1-(2,4-dinitrophenyl)-3-carbamoylpyridiniumchloride, H_2O. [**e**] $(CH_3O)_3PO$, $POCl_3$, 0 °C. [**f**] Ac_2O, pyr, 10 °C. [**g**] **6**, DMF/pyr.

Their synthesis started from D/L-ribofuranosylamine **2**, which was prepared on multigram-scale by adopting three literature procedures. The route commenced with a Diels-Alder reaction between achiral cyclopentadiene and tosylcyanide, followed by acidic hydrolysis, to produce **1**[39]. After the *cis*-dihydoxylation and lactam methanolysis of **1**, as described by Cermak *et al*.[40], the sequance is finalized by reduction of the methyl ester[41], providing racemic ribofuranosylamine **2** in 76% yield over three steps. From here, the nicotinamide moiety could be introduced via application of the Zincke reaction, reacting the secondary amine in **2** with 1-(2,4-dinitrophenyl)nicotinamide chloride.[42] Selective phosphorylation of the primary alcohol, by treatment with phosphoryl chloride, lead to produce D/L-**4** as a single product. The coupling of **4** to adenosine monophosphate (AMP) proved to be the most difficult step during the synthesis. Various unsatisfactory coupling conditions were attempted, including Bovine adenylyltransferase catalyzed phosphorylation and Michelson activation. The latter involves the formation of a reactive mixed anhydride between a donor phosphate monoester (e.g. **4**) and diphenyl phosphorochloridate. Controlled substitution of the diphenoxyphosphoryloxy-moiety with an acceptor phosphate leads to the formation of the desired pyrophosphate. Finally, the authors adopted a more

refined iteration of this activation-displacement method, as described by Furusawa *et al.*[43], to successfully couple di-*n*-butylphosphinothioic anhydride **6**, under the agency of silver nitrate, with D/L-*C*-NMN **4**, providing *C*-NAD$^+$ and its respective diastereoisomer. A simple but effective optimization was found in the acetyl protection of the 2,3-diol in **4**. The improved solubility of **5** allowed for the use of more favorable solvent mixtures during the subsequent coupling reaction, significantly improving yield and reproducibility. After ammonia mediated deacylation during work-up, the two diastereoisomeric *C*-NAD analogues could be separated chromatographically. The structures were assigned by exposing both diastereoisomers to yeast and equine liver alcohol dehydrogenases, that naturally use NAD$^+$ as a co-substrate in the oxidation of alcohols. Both enzymes showed activity with the compound that was accordingly assigned as *C*-NAD$^+$, while no enzymatic activity was observed with L-ribosyl-C-NAD$^+$. Although the authors did not evaluate *C*-NAD$^+$ in context of PARPs, it was demonstrated that the analogue was capable of non-covalently inhibiting NAD glycohydrolase from *Bungarus Fasciatus* venom at micromolar concentrations. In 1998, *C*-NAD$^+$ was used by Ruf and co-workers to obtain the first crystal structure of PARP-1 with a NAD$^+$ mimetic bound in the active site.[14]

Benzamide Adenine Dinucleotide. At the beginning of the 1990s the importance of poly-ADP-ribosylation in DNA-repair mechanism was well-established, and PARPs were considered as interesting therapeutic targets in relation to cancer research. However, at this time, no suitable PARP inhibitors were known. In response Krohn *et al.* proposed benzamide riboside (**10**) and benzamide mononucleotide (**11**, Scheme 2), which were predicted to be anabolized intracellularly to the actual envisioned PARP inhibitor and NAD$^+$ analogue; benzamide adenine dinucleotide (BAD, Scheme 3).[44] In this design the riboside ring-oxygen is retained, instead the labile anomeric C^1-N$^+$ bond is removed by substituting the nicotinamide moiety with benzamide.

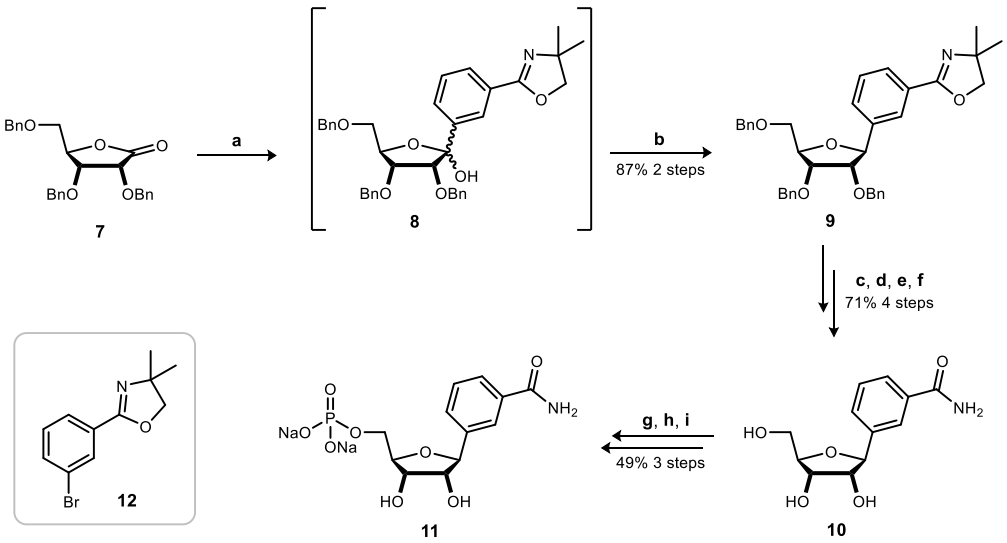

Scheme 2: Synthesis of benzamide mononucleotide as described by Krohn and co-workers. Reagents and conditions: [**a**] *n*BuLi, **12**, THF, -85 °C. [**b**] $BF_3{\cdot}Et_2O$, Et_3SiH, DCM, -78 °C. [**c**] MeI, $MeNO_3$, 100 °C. [**d**] NaOH, MeOH, reflux. [**e**] i: $SOCl_2$, DMF, reflux. ii: NH_4OH. [**f**] Pt/C, H_2, THF. [**g**] Acetone, H_2SO_4, 0 °C. [**h**] $POCl_3$, $PO(OMe)_3$, 0 °C [**i**] HCl, H_2O, 70 °C.

After various investigative reactions and refinements, the final synthesis commenced with the nucleophilic addition of lithiated 3-bromophenyl oxazoline **12** onto benzylated D-ribonolactone **7**. Subsequent silane deoxygenation of the anomeric hydroxyl, in intermediate **8**, afforded protected riboside **9** in stereoselective fashion. Recovery of the amide from the oxazoline moiety and ensuing debenzylation provided benzamide riboside (**10**). To facilitate the installation of the phosphate the 2,3-diol was protected as an isopropylidene acetal. Phosphorylation of the primary alcohol and acidic cleavage of the isopropylidene were carried out in a single operation, yielding target benzamide mononucleotide **11**. As part of their study, Krohn *et al.* evaluated **11** for its biological activity. Although no poly(ADP)ribosylation inhibition was found, **11** showed up to nanomolar level toxicity towards various human tumor cell lines.[45] This potent anti-proliferate activity could indeed be contributed to the anabolic conversion of **11** to BAD, which acted through the inhibition of inosine-5-monophosphate dehydrogenase (IMPDH).

Zatorski and co-workers expanded on the synthesis of BAD (Scheme 3) to determine if the analogue showed selective inhibition between the two IMPDH isoforms (type I and II).[46] Experiencing disappointing yields with the P^V-phosphorylation method reported by Krohn *et al*, the authors turned to a phosphoramidite approach for the preparation of **15**. The reaction of benzamide riboside **13** with 2-cyanoethyl *N*,*N*-diisopropylchlorophosphoramidite, followed by tetrazole mediated installment of the second 2-cyanoethanol and oxidation with *tert*-butyl peroxide, gave the desired dicyanoethyl phosphate. The crude intermediate was treated with methanolic ammonia during work-up, providing phosphate diester **14**. After elimination of the second cyanoethyl, protected benzamide riboside **15** was converted to activated imidazolium species **16** followed by reaction with 2,3-*O*-isopropylidene AMP in a one-pot procedure. Final, acidic deprotection of the isopropylidene groups provided the desired NAD^+ analogue BAD in excellent yield. Unfortunately, BAD did not show selective inhibition between the two isoforms of IMPDH. In 2018, however, Langelier and co-workers established that BAD inhibits the DNA-dependent PARP-1 automodification activity, starting at 50 micromolar concentration.[35] In contrast, *C*-NAD^+ only showed similar levels of inhibition at concentrations twelve times higher. Additionally, the authors were able to obtain the crystal structure of the PARP-1 catalytic domain bound to BAD.

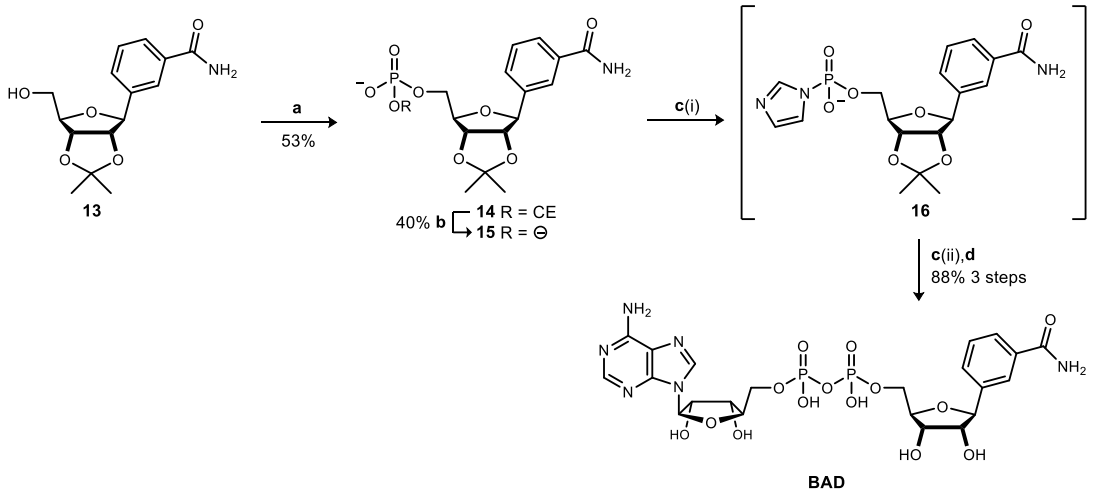

Scheme 3: Synthesis of BAD as described by Zatorski and co-workers. Reagents and conditions: [**a**] i: 2-cyanoethyl *N*,*N*-diisopropylchlorophosphoramidite, DIPEA, DCM. ii: β-cyanoethanol, tetrazole, MeCN. iii: *t*BuOOH. iv: NH_3, MeOH. [**b**] NH_3, MeOH, 55 °C. [**c**] i: CDI, DMF. ii: 2,3-*O*-isopropylidene AMP. [**d**] Dowex-50·H^+, H_2O.

Fluoro-Nicotinamide Adenine Dinucleotide. In the continuous search for NAD^+ analogues Sleath *et al* explored substituting the C^2-*OH* at the nicotinamide riboside.[47] Previous research had shown that the native NAD^+ hydroxyl at the C^2-position participates in base-catalyzed nicotinamide-glycosyl bond cleavage performed by enzymes such as ADP-ribosyltransferases and NAD^+-glycohydrolases. As part of their investigation three arabino-NAD^+ derivatives were synthesized, including fluoro-nicotinamide mononucleotide **25β** and fluoro-NAD^+ analogue ***F*-NAD$^+$** (Scheme 4).

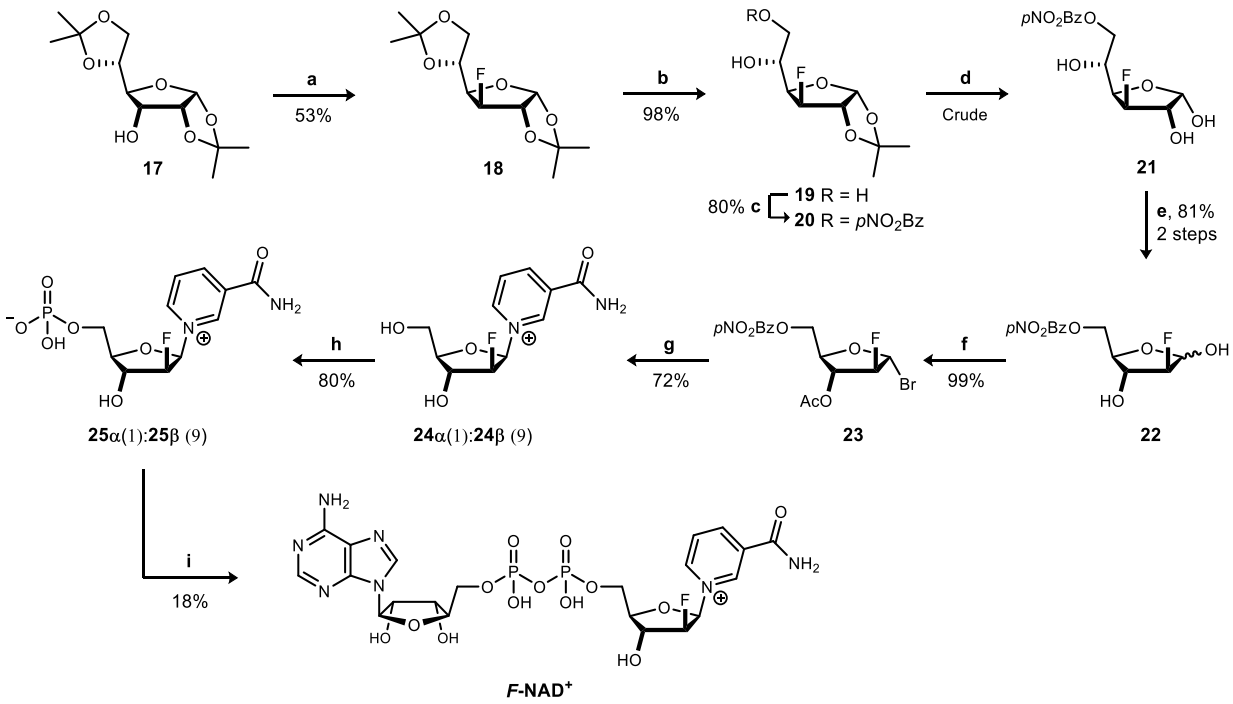

Scheme 4: Synthesis of *F*-NAD^+ as described by Sleath and co-workers. Reagents and conditions: [**a**] DAST, DCM/pyr, 0 °C. [**b**] H_2SO_4, dioxane/ethanol. [**c**] *p*-nitrobenzoyl chloride, DCM/pyr, -30 °C. [**d**] Dowex-50·H^+, dioxane:water, 80 °C. [**e**] $NaHCO_3$, $NaIO_4$, H_2O/MeCN. [**f**] i: Ac_2O, pyr. ii: HBr, AcOH, DCM. [**g**] i: Nicotinamide, MeCN. ii: NH_3, MeOH, 0 °C. [**h**] $POCl_3$, *m*-cresol, 5 °C. [**i**] i: Ac_2O, pyr. ii: $(PhO)_2POCl$, Bu_3N, DMF. iii: AMP, DMF. iv: NH_3, MeOH, 0 °C.

Sleath's synthesis started with DAST mediated fluorination of protected allofuranose **17**, showing typical S_N2-inversion of the stereochemistry. Selective deprotection of the terminal isopropylidene with dilute acid, followed by reprotection of primary hydroxyl with *p*-nitrobenzoyl chloride, provided alloside **20**. Transformation to the arabino-conformation was carried out via an oxidative cleavage method. After removal of the 1,2-*O*-isopropylidene, the produced diol was cleaved with sodium periodate, effectively converting the C^2-*OH* into the (open-chain) anomeric aldehyde, which, upon ring-closure with the original C^5-*OH*, generates the desired fluoro-arabinofuranose **22**. A one-pot acetylation-bromination procedure gave α-bromide **23** in over 95% diastereoisomeric excess. Anomeric displacement of the bromine with nicotinamide and consecutive ammonolysis of the ester-based protecting groups produced primarily beta-anomer **24β**. Separation of the α/β-mixture was postponed until after formation of *F*-NAD^+. To facilitate the solubility of the α/β-nicotinamide nucleotide derivative, the phosphorylation reaction was carried out in *m*-cresol with phosphoryl chloride[48], yielding fluorinated NMN analogue **25α** and **25β** as a diastereoisomeric mixture. The coupling reaction was accomplished via a modified version of the earlier discussed Michelson method, in which the secondary hydroxyl in **25** is acetylated *in situ* to accommodate

for the otherwise poor solubility of the NAD^+ derivative under the succeeding coupling conditions. Activation with diphenyl chlorophosphate and reaction of the activated intermediate with AMP successfully gave a mixture of *F*-NAD^+ and the α-nicotinamide diastereoisomer. *F*-NAD^+ was then isolated by chromatographic separation.

Fluoro-nicotinamides have been applied extensively to study ARTs, including a subclass of enzymes known as ADP-ribose cyclases (ARCs). The best-known ARCs are CD38 and CD157.[49] These transmembrane enzymes are employed by mammalian cells to metabolize NAD^+, generating ADPR and to a lesser extent cyclic ADP-ribose (cADPR).[50,51] The latter is a second messenger that regulates intercellular Ca^{2+} concentrations as part of cell signal transductions. CD38 has become known as a powerful marker for several human hematological tumor cell lines, and is directly involved in various cellular immune response mechanisms.[52] The involvement of CD38 in these type of physiological processes has led to a persistent scientific interest in its catalytic mechanism. In 2000, Sauve and co-workers established the active site's catalytic residue as the side chain carboxylate of glutamic acid 226.[53] This was demonstrated by exposing the enzyme to the above described fluorinated NMN analogue **25β** (Scheme 4), which reacted with Glu_{226} to provide a stable covalent enzyme-inhibitor intermediate, as was determined by mass spectrometry. The electronegative fluorine atom at the C^2-position significantly increases the dissociation energy of the anomeric ester bond towards the oxocarbenium-ion transition state, thereby drastically slowing down the succeeding hydrolysis or cyclization step. In 2010, Zhang *et al* complemented these results by publishing the first X-ray crystal structure of CD38, with irreversible covalent inhibitor *F*-NAD^+ bound to Glu_{226}.[54] By crystalizing *F*-NAD^+ with a Glu_{146}-mutant CD38, it was also discovered that the point removal of this second key residue abolishes CD38s hydrolytic activity, while greatly enhancing its cyclization activity.

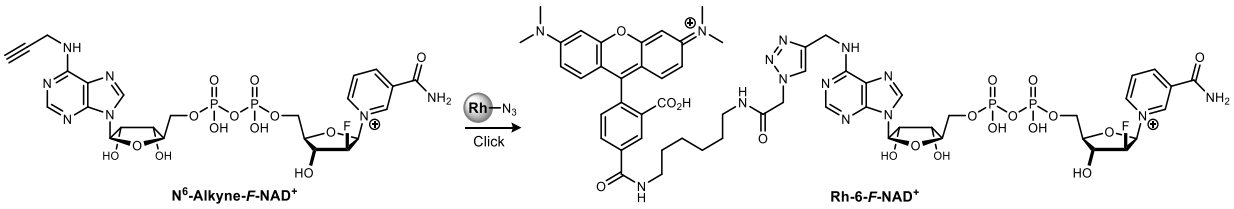

Figure 4: The structure of fluorescent activity-based probe Rh-6-F-NAD^+.

To study the CD38-mediated signal processes, Jiang and co-workers sought to develop a labeling method for the real-time monitoring of the enzyme. To this end they designed and synthesized a fluorescent activity-based probe based on *F*-NAD^+, aiming to take advantage of the covalent nature of the inhibitor.[55] Installation of a propargyl group onto the N^6-position of the adenine moiety enables click-conjugation with an azido bearing fluorophore (Figure 4). In their study Rhodamine was selected at the reporter group of choice. The resulting probe, Rh-6-*F*-NAD^+, successfully labeled CD38 in life cells.

Stabilized ADP-ribosylated Oligopeptides

Ever since poly-ADP-ribosylation of chromatin proteins was discovered to be involved in processes such as DNA-repair, cell division, inflammatory response and aging, there has been a growing interest in understanding these processes at a molecular level. However, the complexity of PARylation has led to scientific controversy regarding the target proteins and, most notably, the nature of the acceptor amino-acid(s). Structurally well-defined ADP-ribosylated oligopeptides were conceived as tools to help elucidate the biochemistry of PARylation. The first chemical synthesis of such constructs was described by van der Heden van Noort *et al* in 2011.[56] They recognized that the main difficulty in constructing the native mono- and poly-ADP-ribosylated peptides would be the chemical compatibility between the anomeric linkage (at the ribosylated amino acid), the pyrophosphate bridge and solid-phase peptide chemistry. The MARylation sites of a mammalian RhoA protein and a heptapeptide, based on the natural occurring *N*-terminus of the human histone, were selected as target molecules for their chemical endeavor. Although the latter is naturally PARylated at the glutamic acid residue, the presence of an anomeric ester bond was considered to be not feasible in the synthesis of the construct. Instead glutamine was incorporated as a bioisostere, having the more stable anomeric amide.

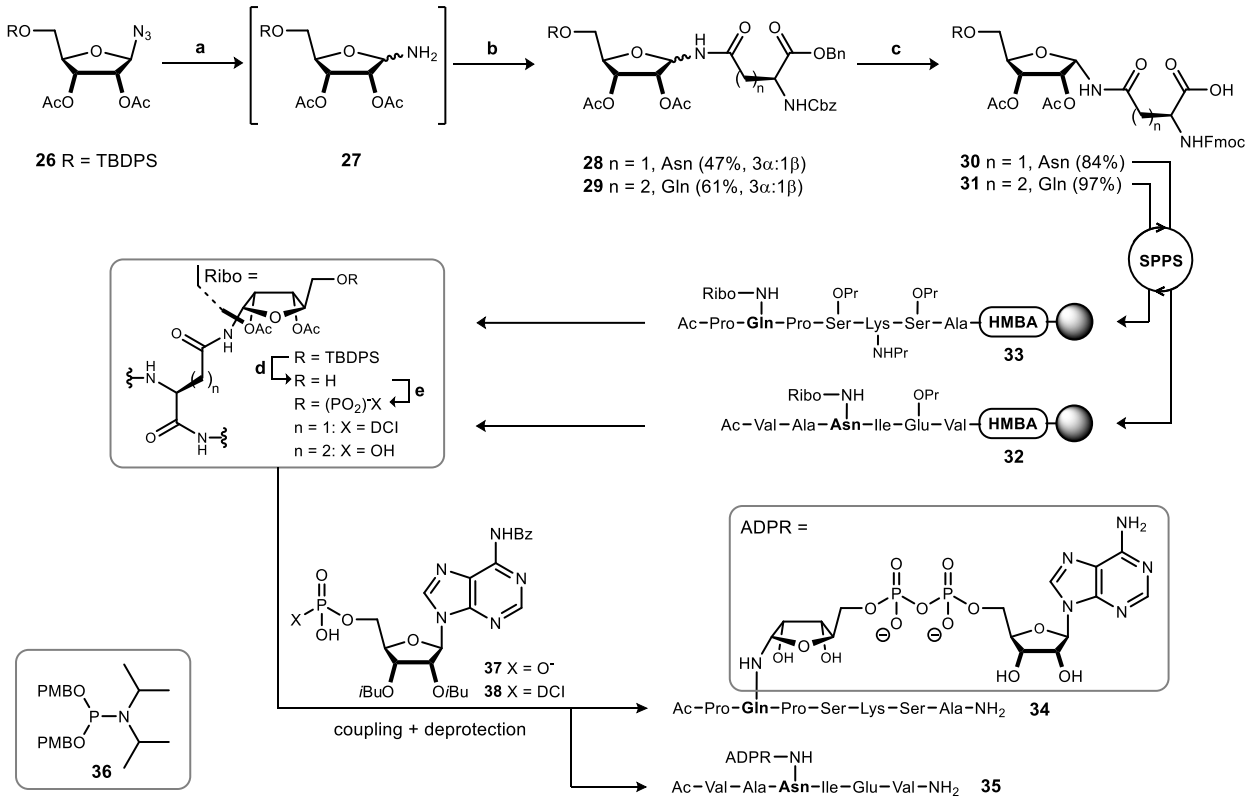

Scheme 5: Synthesis of ADP-ribosylated oligopeptides as described by van der Heden van Noort *et al*. Reagents and conditions: [**a**] PtO_2, H_2, EtOAc, 10 °C. [**b**] Z-Asp-OBn or Z-Glu-OBn, EDC·HCl, DCM. [**c**] i: 10% Pd/C, H_2, MeOH. ii: FmocOSu, $NaHCO_3$, H_2O /acetone. [**d**] HF in pyridine, 0 °C. [**e**] i: **38**, DCI, MeCN, 0 °C. ii: I_2, pyridine, 0 °C for **32** *or* *t*BuOOH ›› TFA for **33**.

A key step in the synthesis entailed the careful hydrogenation of β-azido-riboside **26**, to provide the unstable intermediate hemiaminal ether **27** (Scheme 5). Immediate *in situ* condensation with the corresponding Asn and Gln building blocks gave ribosylated amino acids **28** and **29**, respectively, as α/β-anomeric mixtures. After chromatographically separation, followed by protecting group manipulations, the acquired α-derivatives **30** and **31** were applied as building blocks in a standard solid-phase peptide synthesis. Phosphorylation of the immobilized ribosylated peptides was carried out with di(*p*-methoxybenzyl)-*N*,*N*-diisopropyl phosphoramidite (**36**), using dicyanoimidazole (DCI) as an activator. Constructing the ADPR pyrophosphate bridge for both peptides comprised the same methodology, using a different sequence of event. For ribosylated peptide **32**, iodine mediated oxidation of the installed di-*p*-methoxybenzyl phosphite led to the formation of an phosphorimidazolidate. This immobilized activated phosphate species was then coupled to adenosine monophosphate **37**. Alternatively, for peptide **33**, the introduced phosphite moiety was oxidized with *tert*-butyl hydroperoxide. Cleavage of the *p*-methoxybenzyl groups yielded the terminal phosphate, that was subsequently condensed with adenosine phosphorimidazolidate **38**. The latter approach turned out advantageous as an excess of the activated species could be applied. Global deprotection and release from solid support provided the desired ADP-ribosylated peptides **34** and **35**.

This line of research was continued by Kistemaker *et al*, who refined the strategy by preparing pre-phosphorylated amino acid-riboside building blocks (Scheme 6, **39**-**41**) and applying these in an improved methodology for the on-resin installment of the pyrophosphate.[34] The ribosylated amino-acid building blocks were incorporated into peptide fragments via a standard SPPS protocol to give immobilized ribosylated oligopeptide **42**. Using finely-tuned conditions, the *tert*-butyl groups could be eliminated, leaving the anomeric configuration intact. Next, the pyrophosphate was assembled by adapting the phosphoramidite–phosphonate methodology, as described by Gold and van Delft *et al*,[57] to the synthesis on solid-phase. The immobilized phosphate species **43** was condensed with adenosine phosphoramidite **45** in presence of 5-ethylthiotetrazole as an activator. Oxidation of the phosphite–phosphate intermediate by CSO, followed by global deprotection and concomitant release from solid support, yielded the respective ADP-ribosylated peptide **44**. In this way a multitude of biologically relevant MARylated peptides

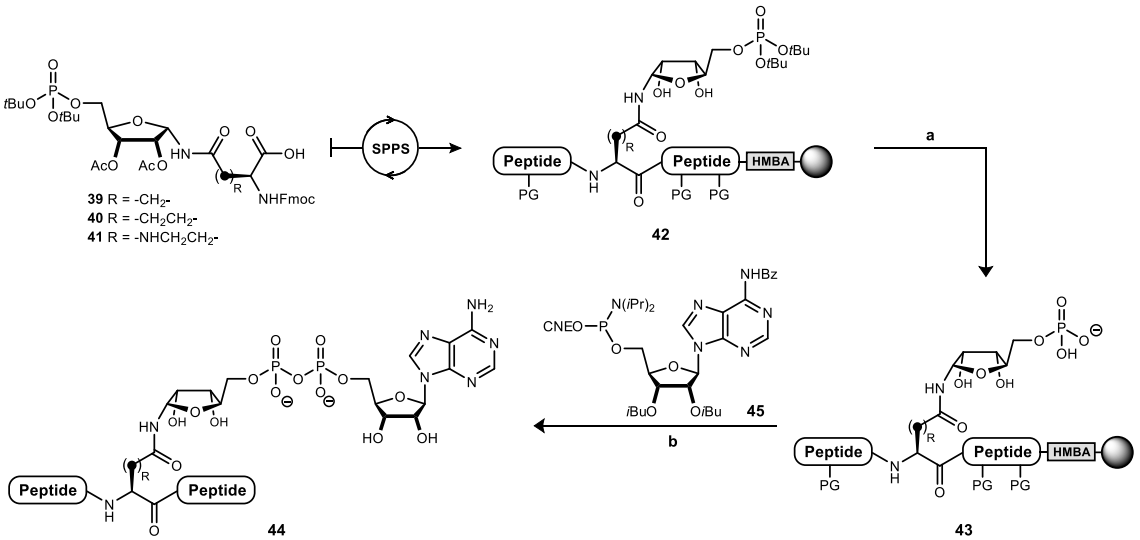

Scheme 6: Synthesis of ADP-ribosylated oligopeptides as described by Kistemaker *et al*. Reagents and conditions: [**a**] i: HCl:HFIP ii: Pyridine [**b**] i: ETT, MeCN ii: CSO, iii: DBU, iv: NH_3, TFE v: NH_4OH.

were synthesized and successfully used to study the substrate specificity of human MacroD2 and TARG1 macro-domains. **Chapter 4** of this thesis describes the synthesis of a mono-ADP-ribosylated H2B conjugate bioisostere wherein a *carba*-riboside is synthetically incorporated to stabilized the peptide-ribose glycosidic bond.

Although the synthesis strategies discussed above were successful in providing several MARylated peptides, each required distinct chemical modifications and highly tailored reaction conditions, and thus are not generally applicable. A practical approach which addressed this limitation was presented by Liu *et al* (Scheme 7).[58] By implementing click-chemistry, they enabled the post-synthetic introduction of the ADPr-moiety onto oligopeptides. First an azide functionalized amino acid is incorporated into the target peptide (**47**) through standard solid phase peptide synthesis. After release from solid support, an α-propargyl configured ADP-ribose building block is installed via the copper catalyzed azide-alkyne cycloaddition (CuAAC), resulting in a triazole-based linkage (**48**). Several derivatives of biologically relevant ADP-ribosylated proteins were prepared this way, including an ADPr-ubiquitin analogue that was phosphorylated naturally during biological evaluation, even though it contained an artificial triazole linkage.

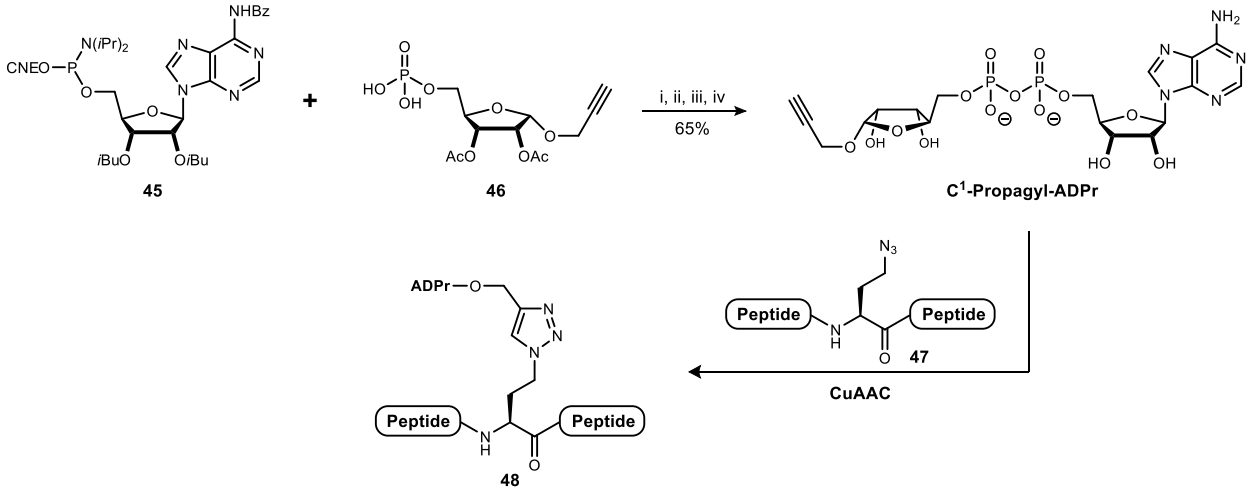

Scheme 7: Click based synthesis of artificial ADP-ribosylated peptides. Reagents and conditions: i: DCI, MeCN ii: *t*BuOOH, iii: DBU, iv: NH_4OH.

Methylene Bisphosphonates

Molecular tools are commonly designed on the basis of functionally relevant natural substrates, intermediates or metabolites. However, care should be taken when reactive or (enzymatically) degradable functionalities are involved in biological process of interest. This also holds true for pyrophosphates. A pyrophosphate moiety within a molecular tool can be considered a labile functionality for both synthesis and biological application, as it is susceptible to hydrolytic or enzymatic degradation. Methylene bisphosphonate are considered stable analogues of pyrophosphates and several common methods for installing these are discussed in the following section.

Terminal Methylene Bisphosphonates. Between 1963 and 1965, Meyers and co-workers published a series of articles on the preparation and implementation of methylene bisphosphates as stabilized

bioisosteres for pyrophosphates (Scheme 8).[59–61] In methylene bisphosphates the oxygen atom conjoining the two phosphates in the original pyrophosphate is replaced by a methylene, providing resistance to cleavage. The synthesis of adenosine methylene diphosphate (me-ADP, **42**) was accomplished by activation of methylenediphosphonic acid with *N*,*N*-dicyclohexylcarbodiimide (DCC), followed by coupling onto adenosine. A similar approach was applied in the synthesis of 2-me-ATP **43**. Here AMP was preactivated with DCC and subsequent condensation with methylenediphosphonic acid gave 2-me-ATP **43**. An alternative method entailing the reaction of adenosine 5-monophosphoramidate with methylenediphosphonic acid also led to the isolation of methylene triphosphate **43**.

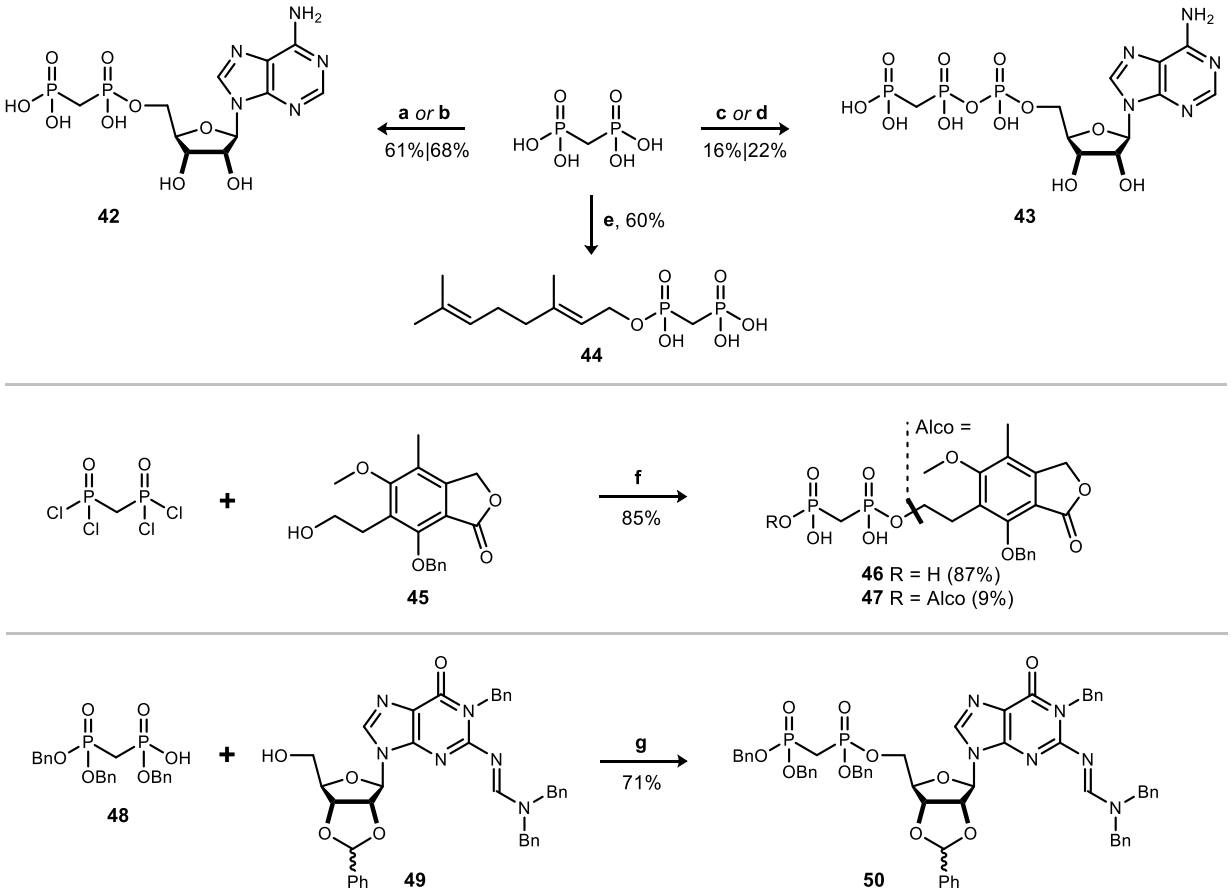

Scheme 8: Exemplified common methods for installing methylene bisphosphates. Reagents and conditions: [**a**] i: 2,3-isopropyl adenosine, DCC, pyr, 60 °C. ii: AcOH/H_2O, 100 °C. [**b**] i: Bu_4NOH, H_2O. ii: 5-tosyl-adenosine, MeCN. [**c**] AMP, DCC, pyr/H_2O. [**d**] Adenosine 5-monophosphoramidate, *o*-chlorophenol, pyr. [**e**] i: Bu_4NOH, H_2O. ii: 1-geranyl chloride, MeCN. [**f**] i: Alco-OH, $(EtO)_3PO$. ii TEAB, H_2O. [**g**] PPh_3, DEAD, THF, 60 °C.

Carbodiimide activation of methylenediphosphonic acid became a well-known strategy for the installation of methylene bisphosphonates. Another procedure to methylenediphosphates include the conversion of a specific alcohol into a leaving group through alkylsulfonation or halogenation and subsequent nucleophilic substitution by anionic methylene diphosphonate (Scheme 8, conditions b and e).[62,63] Alternatively, Lesiak *et al* make use of methylene bisphosphonic(dichloride) to directly phosphorylate alcohol **45** under basic conditions.[64] Upon quenching with water, the trichloromethylene diphosphonate ester intermediate is converted into respective methylenediphosphonic acid **46**. The small discrepancy in

reactivity between formed trichloromethylene diphosphonate ester and unreacted methylene bisphophonic(dichloride) results in the formation of minor amounts of symmetric diester **47**.[65] Hence, symmetric methylene bisphosphonates diesters can be accessed conveniently and in high yields by applying two equivalents of the alcohol instead.[66,67] Each of the discussed strategies install the bisphosphonate moiety in an unprotected fashion, which can be disadvantageous in terms of the solubility degree in common reaction solvents and the ease of purification. In 1998, Vincent and co-workers adopted a reported method for preparing phosphonate mono-esters, using modified Mitsunobu conditions, to the synthesis of guanosine methylene diphosphonate (me-GDP).[68,69] The tribenzylester of methylenediphosphonic acid (**48**) was coupled to the C^5-*OH* of protected guanosine **49** to give fully protected **50** that after silica column purification, reductive global debenzylation provided me-GDP in near quantitative yield.

Unsymmetric Methylene Bisphosphonates. Numerous biologically relevant pyrophosphates are unsymmetric diesters with two different alcohols incorporated; for example NAD^+ and ADPr. In 1986, Meyer and co-workers were the first to synthesize an unsymmetric methylene bisphosphonate bioisostere, based on NAD^+, with the objective to raise antibodies for the detection of ADP-ribose conjugates.[70] me-NAD^+ (Figure 5) was prepared by coupling me-ADP **51** with 2,3-*O*-isopropylidene nicotinamide riboside using the earlier described DCC coupling conditions, followed by acidic deprotection. At the same time, Marquez *et al* implemented the methylene bisphosphonate moiety in an effort to further enhance the effectiveness of known antitumor agent thiazole-4-carboximade adenine dinucleotide (TAD), using identical coupling conditions.[71] In both cases the yields were relatively low; 20% and 36% respectively. Mechanistic study of the DCC-coupling reaction by Pankiewicz and co-workers

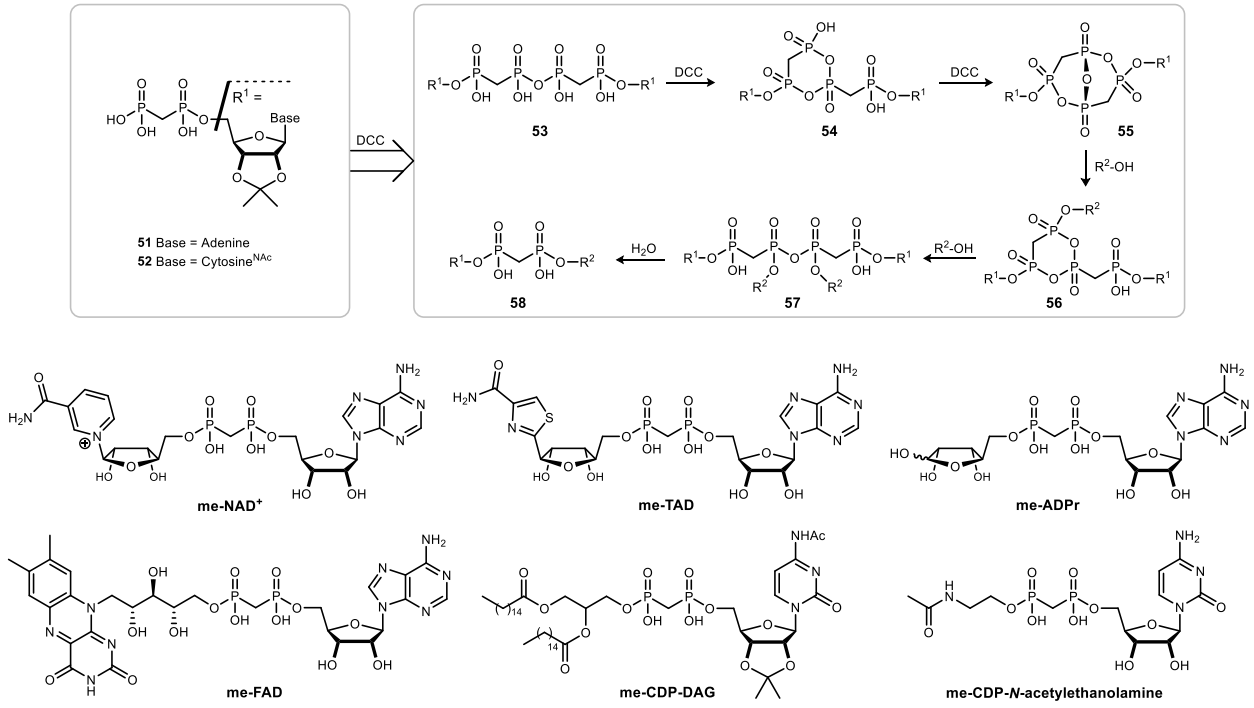

Figure 5: Outlined in grey: The mechanism behind the formation of unsymmetric methylene bisphosphonate nucleotides via carbodiimide activation. Below: An overview of unsymmetric methylene bisphosphonate bioisosteres prepared via DCC coupling. With the exception of me-NAD^+, each of these were prepared by Pankiewicz *et al* using the appropriate acceptor building blocks, in order: 2,3-*O*-isopropyl thiazofurin, 2,3-*O*-isopropyl D-ribose, riboflavin, 1,3-dipalmitoyl glycol, *N*-acetylethanolamine.

revealed that me-ADP dimerizes rapidly upon activation with stoichiometric DCC, forming the corresponding tetraphosphonate analogue (i.e. **53**). The dimer was isolated and proved to be unreactive towards alcohols. This guided them to investigate alternative reaction pathways towards the formation of unsymmetric diesters. ^{31}P NMR spectroscopy revealed that tetraphosphonate **53** could undergo a second and third DCC-activation, followed by two respective intramolecular condensation reactions, giving rise to bicyclic intermediate **55**. Addition of an acceptor alcohol to **55** at 60 °C allows for nucleophilic attack on either bispyrophosphonic position (**56**). Iteration of this reaction on the remaining bispyrophosphonate leads to tetraester **57**, which is effectively the pyrophosphoric dimer of the desired (un)symmetric methylene bisphosphonate. Hence, final hydrolysis of **57** by the addition of water produces two equivalents of methylene bisphosphonate **58**. By implementing these findings into an improved procedure, five unsymmetric methylene bisphosphonates were prepared; me-TAD, me-ADPr, me-FAD, me-CDP-DAG and me-CDP-*N*-acetylethanolamine. In 1999, Ikeda reported an adaptation of Vincent's Mitsunobu methodology for the synthesis of phosphor-protected unsymmetric methylene bisphosphonates.[72] After coupling tribenzyl methylene phosphonate ester **48**, the acquired thiazofurin tetraester could selectively be mono-debenzylated at the terminal phosphonate using stoichiometric amounts of DABCO in refluxing toluene. This set the stage for the installment of an adenosine building block, using the same Mitsunobu conditions, yielding fully protected me-TAD in 72% yield. The carbodiimide and Mitsunobu activations have become established coupling methods for the synthesis of both terminal and unsymmetric methylene bisphosphonates. However, the conditions these methods impose were considered too constraining when it came to the synthesis of methylene bisphosphonate analogues of complex biomolecules such as poly-ADP-ribose fragments. Therefore, an improved methodology for the synthesis of terminal-, symmetric- and unsymmetric methylene bisphosphonates could facilitate PARylation related research. New reagents and complimentary methodology to this end are described in detail in **Chapter 2** and **Chapter 3** of this thesis.

NAD$^+$ Analogues in PARylation Target Labeling

NAD$^+$ analogues functionalized with a ligation handle have been developed and employed in the mapping of ADP-ribosylation activity. The analogues that are accepted as cofactors by a PARP will be metabolically incorporated, carrying over the ligation handles to the produced ADPr-polymer, thereby enabling the visualization of the ADP-ribosylated protein via bioorthogonal labeling. This was first demonstrated by the group of Lin, who used 6- or 8-*N*-propargyl-NAD$^+$ to study PARP-1 activity *in vitro* (Figure 6).[73] Thirty minute incubation of ssDNA with either *N*-propargyl-NAD$^+$ was followed by click-chemistry conjugation of an azido-bearing Rhodamine label. After SDS-PAGE, this allowed for Western blot analysis of tagged auto-ADP-ribosylated PARP-1. In a similar manner, the more efficient 6-*N*-propargyl-NAD$^+$ was employed to label over 70 PARP-1 PARylation substrate proteins. Complimentary results were found by the group of Marx using a 2-alkyne-NAD$^+$ analogue to visualize the PARylation of PARP-1 and Histone H1.2.[74] Complete removal of the modified adenosine C^2-*OH* resulted, as expected, in total loss of poly-ADP-ribose assembly, while deletion of the C^3-*OH* only leads to diminished PAR formation. Small handle modifications were tolerated at the 6-position of adenine, but most optimal were modifications at the 2-position, at which even bulky substituents are accepted.[75] Two accordingly fitted NAD$^+$ analogues, using a cyclooctyne for strain-promoted azide-alkyne cycloaddition ligation and a cyclopropene for the inverse-electron-demand Diels–Alder ligation, were successfully applied in the intracellular visualization of DNA damage induced PARylation.

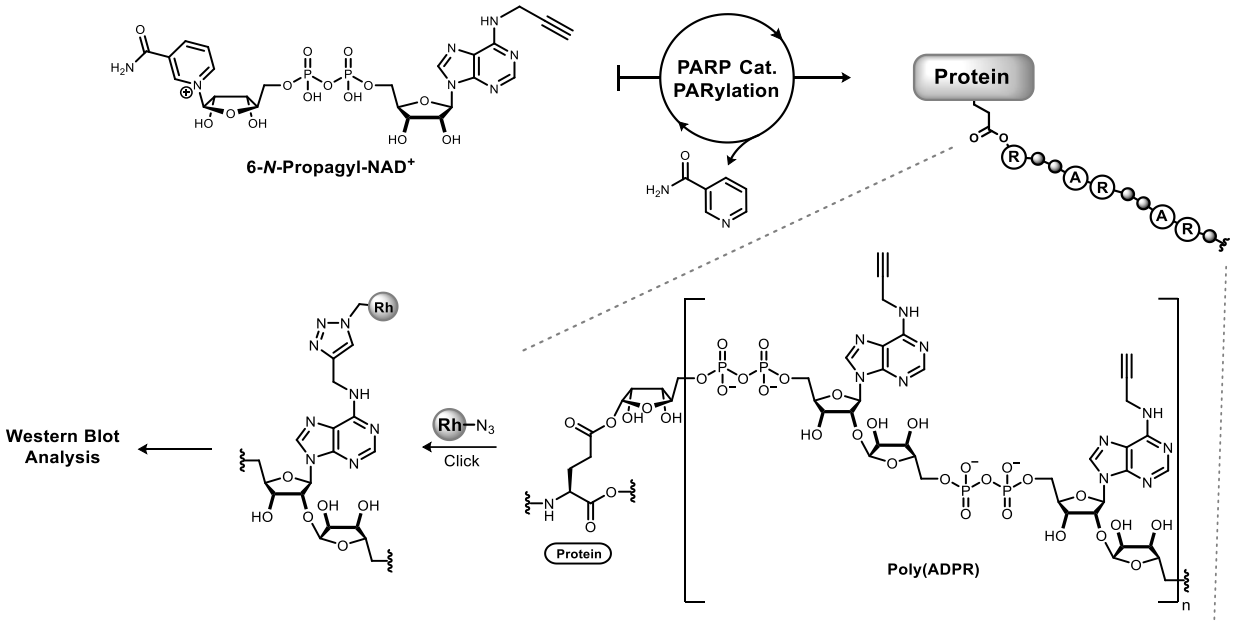

Figure 6: The labeling of PARylated proteins exemplified with 6-*N*-propagyl-NAD$^+$ as reported by the team of Lin. The propargyl bearing NAD$^+$ analogue is metabolically incorporated into the ADPr-polymer. A rhodamine reporter-group is then linked using click chemistry, allowing for Western Blot analysis.

Although global identification of PARylation targets had been achieved through use of handle fitted NAD$^+$ analogues, identifying specific PARylation targets for each of the 17 PARP members remained complicated due to their unanimous use of NAD$^+$ as a cofactor. Cohen and co-workers presented an elegant solution by engineering individual PARP binding pockets to match an orthogonally attuned NAD$^+$ analogue.[76] Based on the crystal structure of substrate-bound PARP-1, it was established that mutating Lys_{903} to an alanine would create a unique hydrophobic pocket. A complementary ethyl substituent at the C^5-position on the nicotinamide moiety was installed to achieve specific pairing with the engineered PARP. Using this analogue-sensitive strategy, 42 PARylation targets were identified for PARP-1 and 301 for PARP-2, with a 52% and 7% respective target overlap. The group of Kraus reported a similar analogue-sensitive approach.[77] The 8-position of the adenine moiety was instead selected as the modification site, as substituents at this position are poorly tolerated by wild-type PARPs. A library of 11 NAD$^+$ analogues were synthesized bearing various R-groups at the 8-position and screened against 20 PARP-1 mutants. From the data it was deduced that mutating Leu_{877} to alanine would result in the desired analogue-sensitivity. Modifying the 8-position of the adenine had the additional advantage that the introduced R-group could simultaneously bear function as a ligation handle. With this in mind, clickable 8-Bu(3-yne)T-NAD$^+$ was designed as the complementary analogue for asPARP-1. Moreover, this particular analogue also demonstrated activity with similarly engineered asPARP-2 and asPARP-3 mutants. Interestingly, 167 protein targets were found for PARP-1, 87 for PARP-2 and 401 for PARP-3, which differs significantly from the findings of Cohen. A reason for this discrepancy was not discussed in the article, but a possible explanation is that the mutations affect protein targeting.

Bioorthogonal Ligation

The field of bioorthogonal chemistry aims to develop chemical reactions that are applicable *in vivo* without affecting natural occurring biochemical processes. In order to do so effectively, the artificially introduced reactive moieties have to be inert to the diverse spectrum of functional groups that reside in a biological system, while still demonstrating specific reactivity towards each other. In addition, a bioorthogonal reaction must be tolerable to aqueous conditions and physiological pH, while displaying sufficiently fast kinetics for the reaction to proceeds rapidly at sub-micromolar concentrations, as this is desired for most biological labeling experiments. Bioorthogonal reactions have made a significant impact to the field of molecular biology, granting tools to study glycosylation chemistry in living cells and animals[78], enable the conjugation of functional moieties to therapeutically relevant proteins[79], and facilitate the *in vivo* assembly of imaging agents.

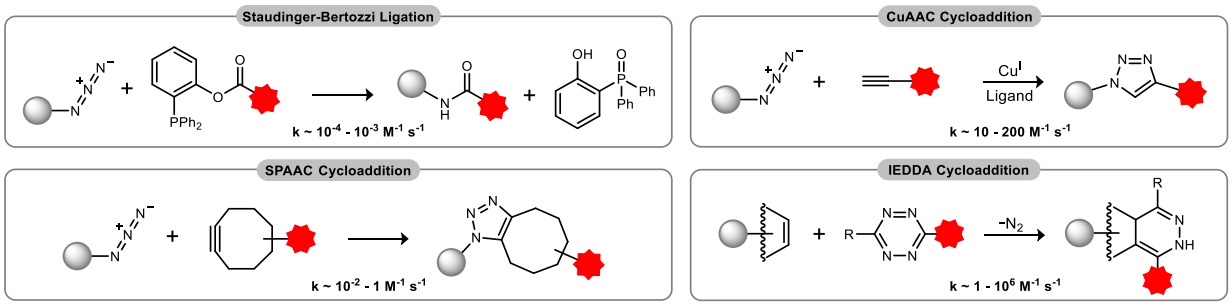

Figure 7: Examples of bioorthogonal reactions used as labeling and conjugation strategies and their relative approximate rates.

Several (pseudo) bioorthogonal two-step labeling techniques have been developed, the most established methods of which are (Figure 7); Staudinger–Bertozzi ligation[80], Cu^{I}-catalyzed alkyne–azide cycloaddition (CuAAC)[81,82], Huisgen strain-promoted alkyne–azide cycloadditions (SPAAC)[83,84] and inverse-electron-demand Diels–Alder reaction (IEDDA).[85] Except for the last, each of these methods utilizes the azide functionality. Azides have virtually no precedence among biomolecules and show exceptional biocompatibility. The groups isoelectric nature allows it to act as both an electrophile and a nucleophile, which enables participation in a wide variety of reactions, often thermodynamically driven by the expulsion of nitrogen. Staudinger–Bertozzi ligation applies an *o*-triarylphosphine benzoate handle to react with an azide functionalized (bio)molecule. After nucleophilic attack of the phosphine onto the azide, the intermediate aza-ylide cyclizes onto the adjacent ester to covalently link the azide substituent in the form of an amide bond. The reaction has been used to label biomolecules in cells and living animals.[86,87] The primary disadvantage of the Staudinger–Bertozzi ligation are the relative slow reaction kinetics, with a second order rate constant of approximately 10^{-3} M^{-1} s^{-1}.[88] Secondly, the *o*-triarylphosphine benzoate moiety is susceptibility to oxidation and enzymatic cleavage.

Ligation strategies based on alkyne-azide [3 + 2] cycloadditions comes in two variation; CuAAC and SPAAC. The reactions are similar in that they conjoin the two reaction partners by producing a triazole linkage. The first entails the reaction of an azide with a terminal alkyne, catalyzed by Cu^{I} salts. The reaction displays considerably faster kinetics than the Staudinger–Bertozzi ligation (± 10 – 200 M^{-1} s^{-1})[89], but cannot be considered fully bioorthogonal because of the reliance on a cytotoxic copper catalyst. The SPAAC variant utilizes ring strained cyclooctynes to accelerate the alkyne-azide reaction into a bioorthogonally acceptable range without depending on a copper catalyst, demonstrating rate constants of 10^{-2} to 1 M^{-1}

s^{-1}.[90] The hydrophobic nature of the cyclooctyne moiety can, however, negatively affect water solubility of the often already lipophilic reporter groups. Both CuAAC and SPAAC have been used to label biomolecules within complex biological systems, including living mammalian cells and animals.[91–93]

The IEDDA reaction is the most recent addition to bioorthogonal reactions. It involves a Diels–Alder reaction between an electron deficient tetrazine (diene) and strained alkene or alkyne. The initial [4+2]-cycloaddition results in a highly strained bicyclic intermediate, consisting of two fused six-membered rings. Driven by the elevation of ring strain, the adduct undergoes a retro-Diels–Alder reaction to expulse nitrogen. Alkene dienophiles afford the corresponding 4,5-dihydropyridazine, while alkynes yield the respective pyridazines.

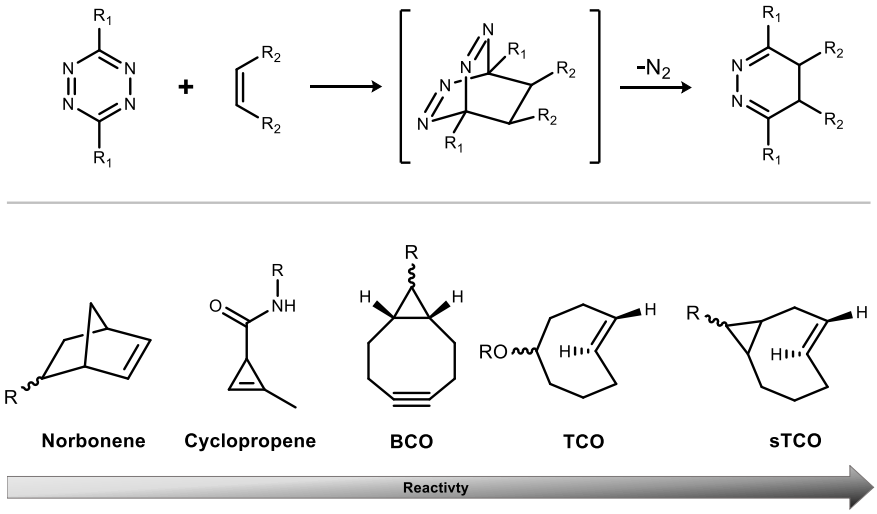

Figure 8: Top: The mechanism of the IEDDA reaction. Bottom: In order of increasing reactivity, five strained alkenes that have been applied as tetrazine reaction partners for the IEDDA-based ligation strategy.

The IEDDA reaction rates are affected by electronic effects of the substituents in the reaction partners, dienophile ring strain and steric effects. For the tetrazine reactant, electron withdrawing substituents lower the LUMO energy and thereby accelerate the reaction rate, whereas electron donating substituents adjacent to the dienophile act conversely by raising the respective HOMO energy.[94–96] Ring strain plays an even more profound role in determining the reaction rate constants. The increase in reactivity caused by this phenomena is two-sided. Firstly, strain heightens the dienophiles HOMO energy and as a result the reaction rate constant. This was empirically substantiated by Saur *et al* who demonstrated that the rate constant correlated with ring strain in the following order: cyclopropene › cyclobutene › cyclopentene › cyclohexene › cyclooctene.[97] The most highly reactive dienophiles were found to be *trans*-cyclooctenes (TCO), however, which have a lower degree of ring strain than for example the less reactive cyclopropenes. A computational study by Houk *et al* endorsed these findings, and additionally exposed that the structural distortion, caused by the adopted TCO crown conformation, mimics the transition state geometry.[98] Consequently, significantly less distortion energy is required for the dienophile to enter a productive transition state, increasing the rate constant. Installing an opposing cyclopropane in TCO forces the ring from a crown conformation to a half-chair conformation, further lowering the distortion energy required, thereby enhancing the reaction rate 160-fold.[99]

Steric effects induced by substituents on either tetrazine or dienophile side have similar dampening effect on reactivity, which can be contributed to both steric repulsion and raised distortion energies. Overall, the IEDDA reaction exhibiting the fastest reaction kinetics among bioorthogonal reactions, with reported rate constants of up to 10^6 M^{-1} s^{-1}. The main drawback of the IEDDA ligation strategy is that both the tetrazine and most reactive dienephiles are relative lipophilic and sterically encumbered. These properties may influence the water solubility and biological response of the functionalized molecules. **Chapter 5** describes the synthesis, reaction kinetics and biochemical implementation of *N*-acylazetines as compact hydrophilic ligation handles for the IEDDA-based bioorthogonal strategy. While **Chapter 6** delves further into the reaction kinetics, isolating the effects of electron induction and ring strain on the dienophilicity of acylenamines.

References

1. P. A. Levene, *J. Biol. Chem.* **1919**, *40*, 415–424.
2. F. Lipmann, *Bacteriol. Rev.* **1953**, *17*, 1–16.
3. P. E. Stein, A. Boodhoo, G. D. Armstrong, S. A. Cockle, M. H. Klein, R. J. Read, *Structure* **1994**, *2*, 45–57.
4. C. Schleberger, H. Hochmann, H. Barth, K. Aktories, G. E. Schulz, *J. Mol. Biol.* **2006**, *364*, 705–715.
5. S. Han, A. S. Arvai, S. B. Clancy, J. A. Tainer, *J. Mol. Biol.* **2001**, *305*, 95–107.
6. C. E. Bell, D. Eisenberg, *Biochemistry* **1996**, *35*, 1137–1149.
7. R.-G. Zhang, D. L. Scott, M. L. Westbrook, S. Nance, B. D. Spangler, G. G. Shipley, E. M. Westbrook, *J. Mol. Biol* **1995**, *115*, 563–573.
8. M. O. Hottiger, P. O. Hassa, B. Lüscher, H. Schüler, F. Koch-Nolte, *Trends Biochem. Sci.* **2010**, *35*, 208–219.
9. G. Glowacki, R. Braren, K. Firner, M. Nissen, M. Kühl, P. Reche, F. Bazan, M. Cetkovic-Cvrlje, E. Leiter, F. Haag, et al., *Protein Sci.* **2009**, *11*, 1657–1670.
10. S. Laing, M. Unger, F. Koch-Nolte, F. Haag, *Amino Acids* **2011**, *41*, 257–269.
11. J. D. Steffen, J. R. Brody, R. S. Armen, J. M. Pascal, *Front. Oncol.* **2013**, *3*.
12. B. A. Gibson, W. L. Kraus, *Nat. Rev. Mol. Cell Biol.* **2012**, *13*, 411–424.
13. S. Vyas, I. Matic, L. Uchima, J. Rood, R. Zaja, R. T. Hay, I. Ahel, P. Chang, *Nat. Commun.* **2014**, *5*, 4426.
14. A. Ruf, V. Rolli, G. De Murcia, G. E. Schulz, *J. Mol. Biol.* **1998**, *278*, 57–65.
15. Y. Zhang, J. Wang, M. Ding, Y. Yu, *Nat. Methods* **2013**, *10*, 981–984.
16. R. K. Morgan, M. S. Cohen, *ACS Chem. Biol.* **2015**, *10*, 1778–1784.
17. G. T. Marsischky, B. A. Wilson, R. J. Collier, *J. Biol. Chem.* **1995**, *270*, 3247–3254.
18. E. Barkauskaite, G. Jankevicius, I. Ahel, *Mol. Cell* **2015**, *58*, 935–946.
19. R. Martello, A. Mangerich, S. Sass, P. C. Dedon, A. Bürkle, *ACS Chem. Biol.* **2013**, *8*, 1567–1575.
20. A. Pines, M. G. Vrouwe, J. A. Marteijn, D. Typas, M. S. Luijsterburg, M. Cansoy, P. Hensbergen, A. Deelder, A. de Groot, S. Matsumoto, et al., *J. Cell Biol.* **2012**, *199*, 235–249.
21. P. Reynolds, S. Cooper, M. Lomax, P. O'Neill, *Nucleic Acids Res.* **2015**, *43*, 4028–4038.
22. S. Petrucco, *Nucleic Acids Res.* **2003**, *31*, 6689–6699.
23. M. Langelier, P. Adp-ribosyl, J. L. Planck, S. Roy, J. M. Pascal, *Structure* **2012**, *728*, 728–733.
24. I. Gibbs-Seymour, P. Fontana, J. G. M. Rack, I. Ahel, *Mol. Cell* **2016**, *62*, 432–442.
25. G. G. Poirier, G. de Murcia, J. Jongstra-Bilen, C. Niedergang, P. Mandel, *Proc. Natl. Acad. Sci. U. S. A.* **1982**, *79*, 3423–3427.
26. K. W. Caldecott, S. Aoufouchi, P. Johnson, S. Shall, *Nucleic Acids Res.* **1996**, *24*, 4387–4394.
27. S. Messner, M. Altmeyer, H. Zhao, A. Pozivil, B. Roschitzki, P. Gehrig, D. Rutishauser, D. Huang, A. Caflisch, M. O. Hottiger, *Nucleic Acids Res.* **2010**, *38*, 6350–6362.
28. Y. Zhang, J. Wang, M. Ding, Y. Yu, *Nat. Methods* **2013**, *10*, 981–984.
29. F. Rosenthal, P. Nanni, S. Barkow-Oesterreicher, M. O. Hottiger, *J. Proteome Res.* **2015**, *14*, 4072–4079.
30. O. Leidecker, J. J. Bonfiglio, T. Colby, Q. Zhang, I. Atanassov, R. Zaja, L. Palazzo, A. Stockum, I. Ahel, I. Matic,

Nat. Chem. Biol. **2016**, *12*, 998–1000.
31. J. M. Pleschke, H. E. Kleczkowska, M. Strohm, F. R. Althaus, *J. Biol. Chem.* **2000**, *275*, 40974–40980.
32. P. L. Panzeter, C. A. Realini, F. R. Althaus, *Biochemistry* **1992**, *31*, 1379–85.
33. P. O. Hassa, S. S. Haenni, M. Elser, M. O. Hottiger, *Microbiol. Mol. Biol. Rev.* **2006**, *70*, 789–829.
34. H. A. V. Kistemaker, A. P. Nardozza, H. S. Overkleeft, G. A. van der Marel, A. G. Ladurner, D. V. Filippov, *Angew. Chemie - Int. Ed.* **2016**, *55*, 10634–10638.
35. M. F. Langelier, L. Zandarashvili, P. M. Aguiar, B. E. Black, J. M. Pascal, *Nat. Commun.* **2018**, *9*, DOI 10.1038/s41467-018-03234-8.
36. A. C. Nottbohm, R. S. Dothager, K. S. Putt, M. T. Hoyt, P. J. Hergenrother, **2007**, *1*, 2066–2069.
37. K. Ueda, O. Hayaishi, *Annu. Rev. Biochem.* **1985**, *54*, 73–100.
38. J. T. Slama, A. M. Simmons, *Biochemistry* **1988**, *27*, 183–193.
39. J. C. Jagt, A. M. van Leusen, *J. Org. Chem.* **1974**, *39*, 564–566.
40. R. C. Cermak, R. Vince, *Tetrahedron Lett.* **1981**, *22*, 2331–2332.
41. B. L. Kam, N. J. Oppenheimer, *J. Org. Chem.* **1981**, *46*, 3268–3272.
42. J. T. Slama, C. Radziejewski, S. R. Oruganti, E. T. Kaiser, *J. Am. Chem. Soc.* **1984**, *106*, 6778–6785.
43. K. Furusawa, M. Sekine, T. Hata, *J. Chem. Soc. Perkin Trans. 1* **1976**, 1711–1716.
44. K. Krohn, H. Heins, K. Wielckens, *J. Med. Chem.* **1992**, *35*, 511–517.
45. G. Kamran, P. K. D., K. J. A., B. J. J., M. V. E., C. D. A., M. Anne, S. Dominic, K. Karsten, J. H. N., *Int. J. Cancer* **1994**, *56*, 892–899.
46. A. Zatorski, K. A. Watanabe, S. F. Carr, B. M. Goldstein, K. W. Pankiewicz, *J. Med. Chem.* **1996**, *39*, 2422–2426.
47. A. L. Handlon, N. J. Oppenheimer, P. R. Sleath, *J. Org. Chem.* **1991**, *56*, 3608–3613.
48. K. ichi Imai, S. Fujii, K. Takanohashi, Y. Furukawa, T. Masuda, M. Honjo, *J. Org. Chem.* **1969**, *34*, 1547–1550.
49. A. Czura, C. Czura, *Mol. Med.* **2006**, *12*, 1.
50. H. Kim, E. L. Jacobson, M. K. Jacobson, *Science (80-.).* **1993**, *261*, 1330 LP – 1333.
51. M. Howard, J. C. Grimaldi, J. F. Bazan, F. E. Lund, L. Santos-Argumedo, R. M. Parkhouse, T. F. Walseth, H. C. Lee, *Science (80-.).* **1993**, *262*, 1056 LP – 1059.
52. S. Partida-Sánchez, D. A. Cockayne, S. Monard, E. L. Jacobson, N. Oppenheimer, B. Garvy, K. Kusser, S. Goodrich, M. Howard, A. Harmsen, et al., *Nat. Med.* **2001**, *7*, 1209.
53. A. A. Sauve, H. Deng, R. H. Angeletti, V. L. Schramm, *J. Am. Chem. Soc.* **2000**, *122*, 7855–7859.
54. H. Zhang, R. Graeff, Z. Chen, L. Zhang, L. Zhang, H. Lee, Q. Hao, *J. Mol. Biol.* **2011**, *405*, 1070–1078.
55. H. Jiang, J. Congleton, Q. Liu, P. Merchant, F. Malavasi, H. C. Lee, Q. Hao, A. Yen, H. Lin, **2009**, 1658–1659.
56. G. J. Van Der Heden Van Noort, M. G. Van Der Horst, H. S. Overkleeft, G. A. Van Der Marel, D. V. Filippov, *J. Am. Chem. Soc.* **2010**, *132*, 5236–5240.
57. H. Gold, P. Van Delft, N. Meeuwenoord, J. D. C. Codée, D. V. Filippov, G. Eggink, H. S. Overkleeft, G. A. Van Der Marel, *J. Org. Chem.* **2008**, *73*, 9458–9460.
58. Q. Liu, H. A. V Kistemaker, S. Bhogaraju, I. Dikic, H. S. Overkleeft, G. A. van der Marel, H. Ovaa, G. J. van der Heden van Noort, D. V Filippov, *Angew. Chemie Int. Ed.* **2017**, *57*, 1659–1662.
59. T. C. Myers, K. Nakamura, J. W. Flesher, *J. Am. Chem. Soc.* **1963**, *85*, 3292–3295.
60. T. C. Myers, L. N. Simon, *J. Org. Chem.* **1965**, *30*, 443–446.
61. T. C. Myers, K. Nakamura, A. B. Danielzadeh, *J. Org. Chem.* **1965**, *30*, 1517–1520.
62. V. M. Dixit, C. D. Poulter, *Tetrahedron Lett.* **1984**, *25*, 4055–4058.
63. V. J. Davisson, A. B. Woodside, T. R. Neal, K. E. Stremler, M. Muehlbacher, C. D. Poulter, *J. Org. Chem.* **1986**, *51*, 4768–4779.
64. K. Lesiak, K. A. Watanabe, J. George, K. W. Pankiewicz, *J. Org. Chem.* **1998**, *63*, 1906–1909.
65. K. W. Pankiewicz, K. B. Lesiak-Watanabe, K. A. Watanabe, S. E. Patterson, H. N. Jayaram, J. A. Yalowitz, M. D. Miller, M. Seidman, A. Majumdar, G. Prehna, et al., *J. Med. Chem.* **2002**, *45*, 703–712.
66. D. C. Stepinski, D. W. Nelson, P. R. Zalupski, A. W. Herlinger, *Tetrahedron* **2001**, *57*, 8637–8645.
67. D. C. Stepinski, A. W. Herlinger, *Synth. Commun.* **2002**, *32*, 2683–2690.
68. D. A. Campbell, *J. Org. Chem.* **1992**, *57*, 6331–6335.
69. S. Vincent, S. Grenier, A. Valleix, C. Salesse, L. Lebeau, C. Mioskowski, *J. Org. Chem.* **1998**, *63*, 7244–7257.
70. T. Meyer, H. Hilz, *Eur. J. Biochem.* **1986**, *155*, 157–165.
71. V. E. Marquez, C. K. H. Tseng, G. Gebevehu, D. A. Cooney, G. S. Ahluwalia, J. A. Kelley, M. Dalai, R. W. Fuller,

Y. A. Wilson, D. G. Johns, *J. Med. Chem.* **1986**, *29*, 1726–1731.
72. H. Ikeda, E. Abushanab, V. E. Marquez, *Bioorganic Med. Chem. Lett.* **1999**, *9*, 3069–3074.
73. H. Jiang, J. H. Kim, K. M. Frizzell, W. L. Kraus, H. Lin, *J. Am. Chem. Soc.* **2010**, *132*, 9363–9372.
74. Y. Wang, D. Rösner, M. Grzywa, A. Marx, *Angew. Chemie - Int. Ed.* **2014**, *53*, 8159–8162.
75. S. Wallrodt, A. Buntz, Y. Wang, A. Zumbusch, A. Marx, *Angew. Chemie - Int. Ed.* **2016**, *55*, 7660–7664.
76. I. Carter-O'Connell, H. Jin, R. K. Morgan, L. L. David, M. S. Cohen, *J. Am. Chem. Soc.* **2014**, *136*, 5201–5204.
77. B. A. Gibson, Y. Zhang, H. Jiang, K. M. Hussey, J. H. Shrimp, H. Lin, F. Schwede, Y. Yu, W. L. Kraus, *Science (80-.).* **2016**, *353*, 45–50.
78. A. A. Neves, H. Stöckmann, Y. A. Wainman, J. C.-H. Kuo, S. Fawcett, F. J. Leeper, K. M. Brindle, *Bioconjug. Chem.* **2013**, *24*, 934–941.
79. B. Oller-Salvia, G. Kym, J. W. Chin, *Angew. Chemie Int. Ed.* **2018**, *57*, 2831–2834.
80. E. Saxon, C. R. Bertozzi, *Science (80-.).* **2000**, *287*, 2007–2010.
81. V. V Rostovtsev, L. G. Green, V. V Fokin, K. B. Sharpless, **2002**, 2596–2599.
82. C. W. Tornøe, C. Christensen, M. Meldal, *J. Org. Chem.* **2002**, *67*, 3057–3064.
83. R. Huisgen, *Proc. Chem. Soc.* **1964**, 349.
84. N. J. Agard, J. A. Prescher, C. R. Bertozzi, *J. Am. Chem. Soc.* **2004**, *126*, 15046–15047.
85. M. L. Blackman, M. Royzen, J. M. Fox, *J. Am. Chem. Soc.* **2008**, *130*, 13518–13519.
86. H. Ovaa, P. F. van Swieten, B. M. Kessler, M. A. Leeuwenburgh, E. Fiebiger, A. M. C. H. van den Nieuwendijk, P. J. Galardy, G. A. van der Marel, H. L. Ploegh, H. S. Overkleeft, *Angew. Chemie Int. Ed.* **2003**, *42*, 3626–3629.
87. J. A. Prescher, D. H. Dube, C. R. Bertozzi, *Nature* **2004**, *430*, 873.
88. F. L. Lin, H. M. Hoyt, H. van Halbeek, R. G. Bergman, C. R. Bertozzi, *J. Am. Chem. Soc.* **2005**, *127*, 2686–2695.
89. N. J. Agard, J. M. Baskin, J. A. Prescher, A. Lo, C. R. Bertozzi, *ACS Chem. Biol.* **2006**, *1*, 644–648.
90. J. A. Codelli, J. M. Baskin, N. J. Agard, C. R. Bertozzi, *J. Am. Chem. Soc.* **2008**, *130*, 11486–11493.
91. S. I. Presolski, V. Hong, S.-H. Cho, M. G. Finn, *J. Am. Chem. Soc.* **2010**, *132*, 14570–14576.
92. N. J. Agard, J. A. Prescher, C. R. Bertozzi, *J. Am. Chem. Soc.* **2004**, *126*, 15046–15047.
93. J. M. Baskin, J. A. Prescher, S. T. Laughlin, N. J. Agard, P. V Chang, I. A. Miller, A. Lo, J. A. Codelli, C. R. Bertozzi, *Proc. Natl. Acad. Sci.* **2007**, *104*, 16793 LP – 16797.
94. D. L. Boger, R. P. Schaum, R. M. Garbaccio, *J. Org. Chem.* **1998**, *63*, 6329–6337.
95. A. Hamasaki, R. Ducray, D. L. Boger, *J. Org. Chem.* **2006**, *71*, 185–193.
96. J. Sauer, D. K. Heldmann, J. Hetzenegger, J. Krauthan, H. Sichert, J. Schuster, *European J. Org. Chem.* **1998**, *1998*, 2885–2896.
97. F. Thalhammer, U. Wallfahrer, J. Sauer, *Tetrahedron Lett.* **1990**, *31*, 6851–6854.
98. F. Liu, Y. Liang, K. N. Houk, *J. Am. Chem. Soc.* **2014**, *136*, 11483–11493.
99. M. T. Taylor, M. L. Blackman, O. Dmitrenko, J. M. Fox, *J. Am. Chem. Soc.* **2011**, *133*, 9646–9649.